Letters in Applied NanoBioScience
Open-Access Journal (ISSN: 2284-6808)

Article
Volume 15, Issue 1, 2026, 8
https://doi.org/10.33263/LIANBS151.008

Bioactive Peptides from *Cissus quadrangularis*: Isolation, Structural Characterization, and Anticancer Evaluation

Jeevitha Rajavel [1], Suresh Kumarasamy [2], Muthusamy Ranganathan [2], Parameswari Aalagarsamy [3,*]

[1] Research Scholar, Department of Biotechnology, M.G.R.College, Hosur, Affiliated to Periyar University, Salem - 636 011, Tamil Nadu, India.
[2] Department of Biotechnology, M.G.R.College, Hosur, Affiliated to Periyar University, Salem - 636 011, Tamil Nadu, India.
[3] Department of Microbiology, K.R.College of Arts and Science, K.R. Nagar, Kovilpatti, 628 503, Tamil Nadu, India.
* Correspondence: sureshbioteck@yahoo.com;

Received: 18.08.2025; Accepted: 20.02.2026; Published: 30.03.2026

Abstract: *Cissus quadrangularis (L.)*, a medicinal plant of the Vitaceae family, has long been utilized for managing metabolic and inflammatory disorders. In this study, bioactive peptides were extracted from shade-dried stem powder using Tris NaCl buffer and purified sequentially by ammonium sulfate precipitation, dialysis, gel filtration, and high-performance liquid chromatography (HPLC). A prominent peptide fraction eluted at 3.16 min with a yield concentration of 80.7 µg/mL. Protein quantification by the Bradford assay confirmed a high peptide content, and structural characterization by mass spectrometry revealed a molecular ion at m/z 650.229, consistent with a low-molecular-weight bioactive peptide. FTIR and circular dichroism spectra indicated predominant β-sheet secondary structures. Functional assays demonstrated significant cytotoxicity (IC_{50} = 42.3 µg/mL) against cancer cell lines, accompanied by morphological features of apoptosis and DNA fragmentation exceeding 65%, as confirmed by comet analysis. This study is the first to isolate and characterize a β-sheet-rich peptide from *C. quadrangularis* with quantifiable anticancer efficacy, highlighting its novel biochemical profile and therapeutic promise as a plant-derived anticancer agent.

Keywords: *Cissus quadrangularis*; bioactive peptides; anticancer activity; apoptosis; DNA fragmentation.

1. Introduction

Cissus quadrangularis (L.) is a perennial succulent climber of the family Vitaceae, easily identified by its green, fleshy, quadrangular stems with four prominent longitudinal ridges that give the plant its name [1]. The stems are smooth, glabrous, and jointed at nodes, where branching and the formation of tendrils, leaves, or inflorescences occur. Young stems are succulent and adapted for water storage, while older stems become woody at the base [2]. The leaves are simple and ovate but often reduced or shed early, allowing the fleshy stems to carry out photosynthesis, a characteristic adaptation of xerophytic plants [3].

Phytochemical investigations have revealed the presence of flavonoids, triterpenoids, steroids, and glycosides, which account for its wide range of pharmacological activities, including antioxidant, anti-inflammatory, and antimicrobial effects [4–6]. While the plant phytochemical profile has been extensively studied, the peptide composition and bioactivity of

plants remain largely unexplored. In recent years, plant-derived peptides have emerged as potent biomolecules due to their high target specificity, structural stability, and therapeutic efficacy [7]. These peptides play crucial roles in regulating cellular signaling, oxidative balance, and immune defense mechanisms [8]. Moreover, several plant peptides have demonstrated anticancer potential, exhibiting properties such as apoptosis induction, mitochondrial dysfunction, and modulation of pro- and anti-apoptotic proteins [9]. However, no comprehensive studies have reported the isolation, characterization, and anticancer evaluation of peptides from *Cissus quadrangularis (L.)*. Addressing this gap, the present study focuses on extracting and characterizing bioactive peptides from *Cissus quadrangularis (L.)* and assessing their cytotoxic, apoptotic, and genotoxic effects on cancer cells. This work provides a novel insight into the peptide-based therapeutic potential of a traditionally significant medicinal plant, thereby bridging ethnomedicine and modern molecular therapeutics [10]. The objectives include isolating and purifying peptides from the stem, followed by structural and biochemical characterization to determine their molecular properties. Further, the study seeks to evaluate the immunomodulatory and anticancer effects of these peptides using a suitable cancer cell line.

2. Materials and Methods

2.1. Collection of Cissus quadrangularis (L.) stem.

Fresh specimens of *Cissus quadrangularis (L.)* were gathered from farmland in Hosur, located in the Krishnagiri District of Tamil Nadu. The plant specimen was taxonomically identified and authenticated by Dr. P. Vijayakanth, Head, Department of Botany, Arignar Anna College, Krishnagiri - 635 115, India, affiliated to Periyar University. A voucher specimen (No. RGRIT/AAC/2024/041) was deposited in the institutional herbarium for future reference. To start, the collected material was placed in an incubator set to 37°C to eliminate any leftover moisture, and then it was left to air dry. After it was completely dried, the plant material was ground into a fine powder using a laboratory grinder. The powdered samples were then stored in airtight containers and kept at −20°C until they were needed for the experimental analyses.

2.2. Extraction of peptide from the stem of Cissus quadrangularis.

Ten grams of powdered *Cissus quadrangularis (L.)* stem material were used as the starting substrate for peptide extraction. The Tris NaCl buffer was prepared by dissolving 0.1 M Tris(hydroxymethyl)aminomethane and 0.15 M sodium chloride in distilled water, and the pH was adjusted to 7.4 using either 1 N HCl or 1 N NaOH. The buffer was sterilized by autoclaving at 121°C and 15 psi for 15 minutes, cooled, and stored at 4°C until further use. Ten grams of plant powder were suspended in 150 mL of the sterile buffer and thoroughly homogenized to facilitate the release of cellular constituents. The homogenate underwent three freeze-thaw cycles (freezing at −20°C and thawing at 4°C over 3-4 days) to enhance cell lysis and promote peptide extraction. Following this treatment, the mixture was centrifuged at 10,000 rpm for 30 minutes at 4°C. The resulting supernatant was separated and passed through Whatman No. 1 filter paper to remove residual debris. The clear filtrate was stored at 4°C for subsequent experiments.

2.3. Purification of the fractionated peptide.

The crude peptide extract from *Cissus quadrangularis (L.)* underwent an initial purification step using gel filtration chromatography. A silicon-coated glass column measuring 80 × 2 cm, packed with Sephadex G-25, provided a bed volume of 120 cm^3 and a void volume ranging from 36 to 40 cm^3. The column was pre-equilibrated with 0.01 M Tris-HCl buffer and operated at a flow rate of 0.33 ml/min under gravity. Crude extract 10 ml was carefully loaded and subsequently eluted with 20 ml of the same buffer. Fractions of 5 ml each were collected, with larger molecular weight peptides eluting first, followed by smaller ones. To ensure consistency, the separation process was repeated three times with fresh extract. Peptide fractions were identified by monitoring absorbance at 280 nm, and fractions with similar elution profiles were combined for further processing. To enhance peptide concentration, ammonium sulfate was added gradually until 80% saturation was reached, followed by incubation at 4°C for 12–16 hours. Precipitated peptides were recovered by centrifugation at 10,000 rpm for 30 minutes at 4°C, and the resulting pellet was redissolved in 0.01 M ammonium bicarbonate.

To remove salts and other low molecular weight contaminants, the resuspended peptide fraction was subjected to dialysis. A 3 kDa cut-off dialysis membrane (HiMedia) was pre-treated with EDTA and sodium bicarbonate at high temperatures, followed by thorough rinsing with hot and cold distilled water. The peptide fraction was dialyzed against Millipore water with continuous stirring at 4°C for 24 hours, effectively eliminating smaller impurities while retaining the desired peptides. The dialyzed fraction was stored at –20°C until further purification. Separation was carried out using a C18 reverse-phase column connected to an LC-20AD system equipped with a UV detector set at 220 nm. The mobile phase consisted of Solvent A (0.1% trifluoroacetic acid in water) and Solvent B (0.1% trifluoroacetic acid in acetonitrile). The peptides were eluted under a linear gradient of 5% – 80% B over 30 minutes at a flow rate of 1.0 mL min^{-1}, with an injection volume of 20 µL. The system was equilibrated with 5% B for 10 minutes before each run. Collected fractions were freeze-dried and preserved at –20°C for subsequent analysis.

2.4. Purified peptide analysis by MALDI TOF/MS.

The purified peptide was analyzed for molecular weight and ionization using an UltrafleXtreme MALDI TOF mass spectrometer operated in positive ion mode. The instrument was run at 26 kV with appropriate lens settings and a 50 Hz nitrogen laser (337 nm). The peptide sample was mixed with α-hydroxycinnamic acid matrix and co-crystallized before analysis. Upon laser irradiation under vacuum, the matrix absorbed the energy, transferring charge to the peptide, which was then ionized and accelerated. The time of flight of the ions was measured, providing the molecular mass characteristics of the purified peptide. The precursor ion was selected for fragmentation, and the resulting daughter ion spectra were interpreted to determine the amino acid sequence. The generated spectra were compared with known peptide databases using bioinformatics tools.

2.5. Peptide analysis by circular dichroism (CD) spectroscopy.

Far-UV circular dichroism (CD) spectroscopy was performed in the wavelength range of 190–250 nm using a JASCO spectropolarimeter with a path length of 1 mm. Measurements were recorded at ambient temperature with peptide samples prepared at a concentration of 0.2

mg/ml in 10 mM sodium phosphate buffer (pH 7.0). The secondary structural elements of the ascidian peptide, including α-helical and β-sheet contents, were quantitatively evaluated using the K2D2 online platform, which employs a self-organizing map (SOM)-based algorithm for predictive analysis.

2.6. Peptide analysis by FTIR.

Fourier transform infrared (FT-IR) spectra of the purified peptide sample were acquired using a Bruker Alpha spectrophotometer. For analysis, 100 µL of the partially purified peptide solution prepared in phosphate buffer was applied to the photoemitter platform, and spectral data were collected in the range of 4000–650 cm^{-1}, expressed as percent transmittance.

2.7. Cytotoxic potential of peptides by MTT-based assay.

Cells were cultured in Dulbecco's Modified Eagle Medium (DMEM) supplemented with 10% fetal bovine serum (FBS), 1% penicillin, and maintained at 37°C in a humidified 5% CO_2 incubator. For the assay, cells were seeded at a density of 1×10^4 cells per well in 96-well plates and allowed to adhere overnight. The test peptide stock solution (1 mg/mL) was prepared in 0.05% DMSO and diluted with culture medium to obtain final concentrations ranging from 5–100 µg/mL. After 2 h of preincubation, cells were treated with different peptide concentrations for 24 h and 48 h, with untreated cells (medium + 0.05% DMSO) serving as negative controls. Cisplatin (10 µM) was used as a positive control to validate assay performance. Following treatment, 15 µL of MTT solution (5 mg/mL in PBS) was added to each well and incubated for 4 h at 37°C. The resulting formazan crystals were dissolved in 100 µL DMSO, and absorbance was recorded at 570 nm using a microplate reader. All experiments were conducted in triplicate (n = 3) and expressed as mean ± standard deviation (SD). The IC_{50} values (concentration required to inhibit 50% of cell viability) were determined by nonlinear regression analysis using GraphPad Prism 5. Statistical significance between the treated and control groups was evaluated using one-way ANOVA, followed by Dunnett's post hoc test, with $p < 0.05$ considered significant.

2.8. Potential of peptides by ROS production assay.

The production of intracellular ROS in CAL-27 oral cancer cells was measured using the DCFDA/H_2DCFDA assay. Cells were seeded in 96-well plates (1×10^4 cells/well) and incubated for 24 h at 37°C and 5% CO_2. After washing with serum-free DMEM, cells were treated with 20 µM DCFDA for 30 min in the dark. Unbound dye was removed with cold PBS. Fluorescence was recorded using a microplate reader at 485 nm excitation and 535 nm emission, and observed under a fluorescence microscope. Untreated cells served as the negative control, and H_2O_2-treated cells (100 µM, 30 min) were used as the positive control.ROS levels were expressed as relative fluorescence units (RFU) compared to controls. All experiments were performed in triplicate (n = 3), and results were shown as mean ± SD.

2.9. Potential of peptides by apoptosis assay.

Apoptosis was assessed in CAL-27 cells using flow cytometry. Cells were seeded at a density of 1×10^5 per mL in 25 cm^2 T-flasks and allowed to adhere overnight. The cultures were then exposed to varying concentrations of the methanolic extract for 24 hours. To detect apoptotic populations, cells were stained with acridine orange (AO) and ethidium bromide

(EtBr) for 15 minutes under dark conditions. The stained cells were subsequently examined under a fluorescence microscope for apoptotic features.

2.10. DNA fragmentation assay.

CAL-27 cells were incubated with test samples for 24 h, harvested, and lysed in buffer (Tris-HCl, EDTA, Triton X-100) at 4°C for 1 h. Lysates were centrifuged (15,000 rpm, 10–15 min), and the supernatants were treated with proteinase K and RNase I at 50°C for 30 min. DNA was purified by phenol-chloroform extraction, precipitated with sodium acetate and ethanol, and resuspended in TE buffer. The samples were run on 1% agarose gel, stained with ethidium bromide, and visualized under UV light. Comet images were captured under a fluorescence microscope, and parameters such as tail length and tail moment were quantified using CometScore 2.0 software. The degree of DNA fragmentation was expressed as mean ± SD from at least 50 cells per sample.

3. Results and Discussion

3.1. Sequential processing of plant material.

Fresh stems of Cissus quadrangularis (L.) were harvested and prepared for experimental use. After thorough cleaning (Figure 1), the stems were shade-dried and ground into a fine powder. From an initial 1000 grams of fresh material, 100 grams of powdered substance were obtained, corresponding to an approximate recovery of 10% (w/w). This powdered form was subsequently utilized for further analysis.

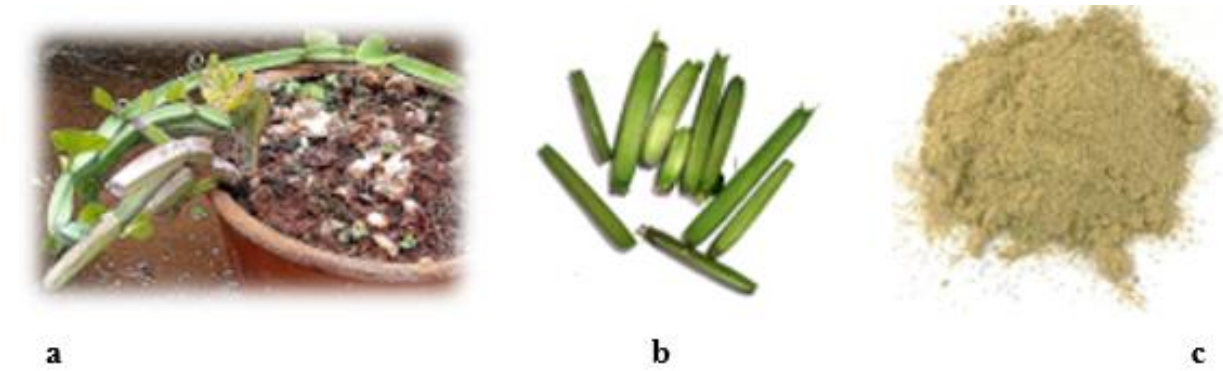

Figure 1. Stages of sample preparation from *Cissus quadrangularis (L.).* **(a)** The whole plant showing quadrangular green stems; **(b)** freshly harvested and cleaned stem segments; **(c)** the shade-dried powdered stem.

3.2. Peptide from the freeze-thaw method.

Peptide extraction from *Cissus quadrangularis (L.)* stem powder using Tris NaCl buffer was successfully carried out. From the initial 10 g of plant powder suspended in 150 ml of buffer, homogenization followed by three freeze–thaw cycles resulted in effective cellular disruption. After centrifugation at 10,000 rpm for 30 minutes at 4°C, approximately 135 ml of clear supernatant was obtained, indicating minimal pellet formation [14]. The supernatant, after filtration through Whatman No. 1 filter paper, yielded 130 ml of debris-free peptide-rich extract, which was subsequently stored at 4°C for purification and characterization experiments.

3.3. Volume of fractionated peptide.

This crude extract represented the maximum soluble peptide content available after homogenization and freeze-thaw cell disruption. For initial purification, 10 ml aliquots of the crude extract were subjected to Sephadex G-25 gel filtration. Fractions of 5 ml were collected, and peptide-containing eluates were identified by UV absorbance at 280 nm. Repeated runs and pooling of similar fractions yielded a combined peptide-rich volume of 25–30 ml, demonstrating efficient separation of higher- and lower-molecular-weight components. Ammonium sulfate precipitation (80% saturation) followed by centrifugation produced a concentrated pellet that, upon redissolving, yielded 12–15 ml peptide solution. This indicated substantial removal of non-precipitating contaminants and a 2-fold reduction in sample volume, reflecting improved peptide enrichment [15,16]. Dialysis of the redissolved fraction through a 3 kDa cut-off membrane further reduced the volume to 10–12 ml, effectively eliminating salts and low-molecular-weight impurities. At this stage, the extract was notably enriched in peptides while retaining structural stability(Figure 2).

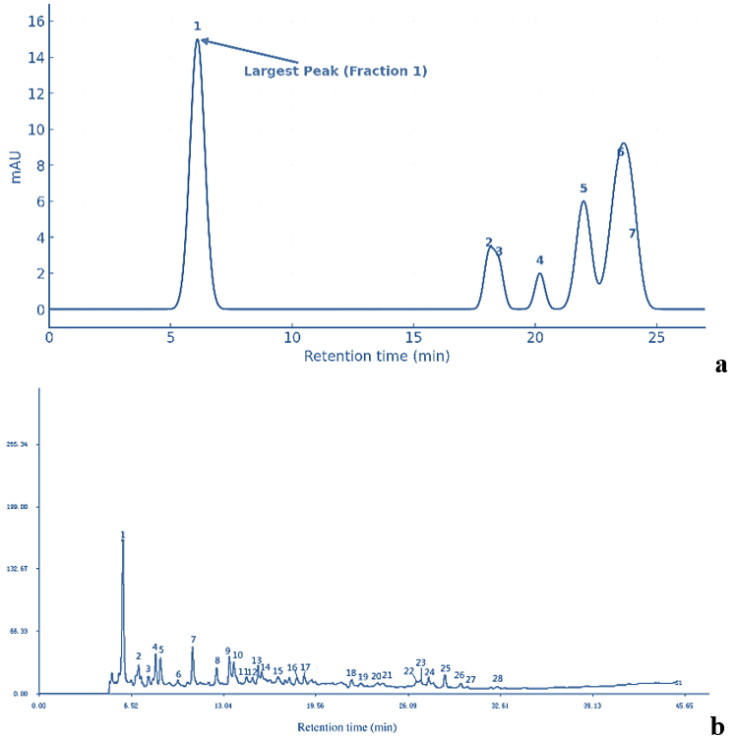

Figure 2. Preparative *HPLC chromatogram* showing multiple fractions. The major peak at 6.1 min (Fraction 1) with 16 mAU represents the **(a)** dominant peptide component; **(b)** reference chromatogram.

Finally, preparative HPLC provided high-resolution separation. Preparative HPLC of the peptide fraction obtained from *Cissus quadrangularis* (L.) yielded multiple peaks at different retention times, indicating separation of distinct peptide components. The chromatogram showed a dominant peak at 6.1 minutes (Fraction 1) with the highest absorbance intensity (16 mAU), representing the major peptide component. In addition to this, several smaller peaks were detected at retention times of ~17.8 min (Fraction 2), 18.9 min (Fraction 3), 19.8 min (Fraction 4), 22.3 min (Fraction 5), 23.9 min (Fraction 6), and 25.1 min (Fraction 7). These peaks correspond to minor peptide species, suggesting that the extract contains a heterogeneous peptide mixture with one abundant peptide fraction. The HPLC profile clearly demonstrates that the peptide extract from *Cissus quadrangularis* comprises multiple peptide fractions that differ in polarity and hydrophobicity [16,17]. The largest and earliest-eluting

peak (Fraction 1 at ~6.1 min) indicates a relatively more polar peptide that interacts less with the hydrophobic stationary phase and elutes quickly. This suggests that Fraction 1 is the major peptide component of the extract and may account for most of the biological activity [18].

3.4. Mass spectrometric analysis of the purified peptide.

Mass spectrometric analysis of the purified peptide fraction from Cissus quadrangularis (L.) revealed several ion peaks within the m/z range of 500–600, along with a prominent peak at m/z 650.229, which corresponded to the molecular weight (MW) of the major peptide component (Figure 3). The additional peaks observed at m/z 523.308, 550.791, 568.286, and 588.272 represent fragment ions or possible minor peptide variants generated during ionization. The precursor ion corresponding to m/z 650.229 was selected for fragmentation, and the resulting daughter ion spectra were interpreted to determine the amino acid sequence. Peptide sequencing analysis confirmed that the major peptide associated with the m/z 650.229 ion possessed the amino acid sequence MESEDHISCLPYTNHVSRSTTVTSLNSHTYTLTFPT EISQR, thereby validating its molecular identity. The generated spectra were compared with known peptide databases using bioinformatics tools, which identified the peptide sequence, confirming its molecular identity. The combined MALDI-TOF/MS and sequencing data confirmed the presence and primary structure of the dominant peptide in the purified fraction. Peptides derived from *Moringa oleifera* (m/z 612–670) and Soybean (m/z 580–690) have been reported to exhibit potent biological activities due to their high content of hydrophobic and sulfur-containing amino acids. Similarly, peptides from *Lupinus albus* and *Pisum sativum* with molecular masses between 600 and 700 Da exhibit strong radical-scavenging and antimicrobial activities, attributed to the presence of histidine, cysteine, and serine residues [19,20].

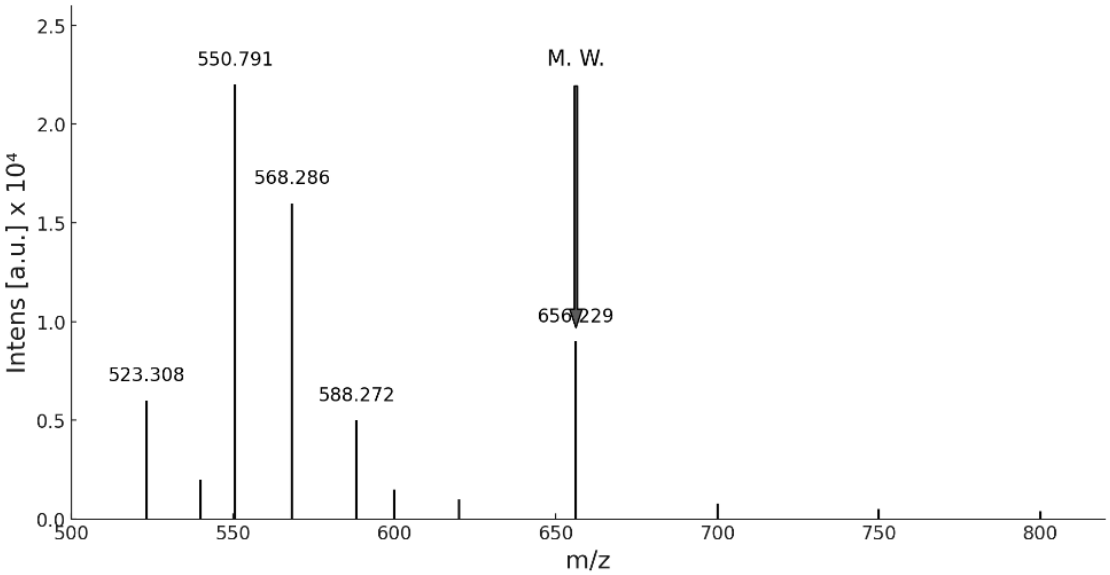

Figure 3. Mass spectrum of purified peptide fraction.

The smaller peaks indicate either partial peptide fragments, post-translational modifications, or less abundant peptide species co-purified during the extraction and chromatography steps [21]. This analysis validates the effectiveness of the purification strategy, which progressively enriched the peptide fraction, as demonstrated by HPLC separation and confirmed here by a clear molecular ion peak. The presence of both a dominant molecular ion and multiple fragment ions suggests that the peptide is stable yet exhibits typical

fragmentation patterns under mass spectrometry [22]. *Cissus quadrangularis* contains a major bioactive peptide of molecular weight 650 Da, accompanied by minor peptide forms.

3.5. Characteristic absorption peaks.

A broad absorption peak around 3300–3400 cm^{-1} indicated the presence of –NH (amide A) stretching vibrations, confirming peptide bonds. The band observed near 2920 cm^{-1} corresponds to C–H stretching vibrations of aliphatic groups (Figure 4). Strong peaks between 1650–1660 cm^{-1} (amide I band) were associated with C=O stretching vibrations, while those around 1540 cm^{-1} (amide II band) represented N–H bending coupled with C–N stretching, both of which are hallmarks of peptide backbones [23]. Additional absorption peaks near 1240–1310 cm^{-1} (amide III band) further supported the peptide structure, corresponding to C–N stretching and N–H deformation. Bands observed around 1050–1100 cm^{-1} could be attributed to C–O stretching vibrations, possibly from hydroxyl-containing amino acid side chains. The FTIR profile thus confirmed the presence of characteristic amide functional groups (amide I, II, and III bands), validating the peptide nature of the purified fraction.

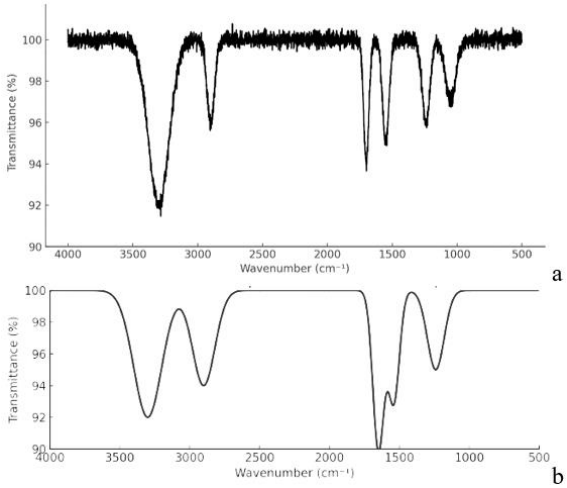

Figure 4. FTIR spectra of **(a)** purified peptide fraction from *Cissus quadrangularis (L.*); **(b)** standard peptide reference showing characteristic amide I, II, and III bands confirming peptide structure.

3.6. CD spectrum validates.

The spectrum showed a strong positive peak near 195 nm followed by a distinct negative band around 210–212 nm, which is characteristic of peptides rich in β sheet structures. The weak shoulder around 200 nm further supports the presence of ordered conformations rather than random coils [24,25]. The absence of a strong double minimum at 208 nm and 222 nm, typical for α-helical structures, suggests that the peptide does not predominantly adopt an α-helical conformation. Instead, the spectral pattern, particularly the positive peak at 195 nm and the negative trough near 210 nm, is consistent with a β sheet-dominated secondary structure with possible random coil contributions (Figure 5).

The identified Cissus quadrangularis peptide (sequence: MESEDHISCLPYTNHVS RSTTVTSLNSHTYTLTFPTEISQR) contains amino acid residues such as methionine, cysteine, histidine, and tyrosine, which are known to participate in redox regulation through hydrogen donation, metal ion chelation, and radical stabilization. These residues may contribute to the peptide antioxidant potential by neutralizing reactive oxygen species (ROS) or preventing lipid peroxidation. Furthermore, the presence of polar and charged amino acids

like serine, threonine, and arginine could enhance solubility and interaction with oxidative enzymes, supporting cellular defense mechanisms.

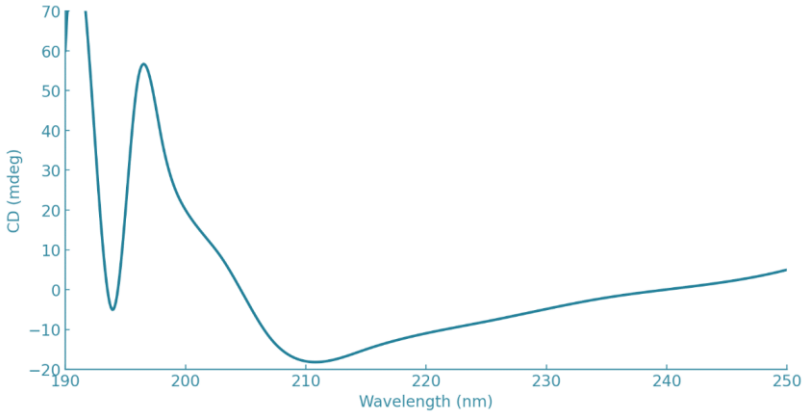

Figure 5. Circular Dichroism (CD) spectrum of purified peptide.

3.7. Dose-dependent cytotoxic effect.

The control group (untreated cells) showed large, intact, and well-distributed spherical green fluorescence, indicating healthy cell morphology and viability. Upon treatment with increasing peptide concentrations, a dose-dependent disruption in cell morphology and fluorescence intensity was observed [26]. At 50 µM, cells began to show early signs of membrane compromise, as evidenced by smaller, scattered fluorescent spots. With 100–150 µM treatment, a marked reduction in intact cell aggregates was noted, accompanied by increased fragmented and punctate fluorescence, suggesting initiation of cell death or lysis (Figure 6). At higher concentrations (200–250 µM), the peptide induced severe morphological disruption, with a large number of cells appearing as small, dispersed fluorescent particles [27].

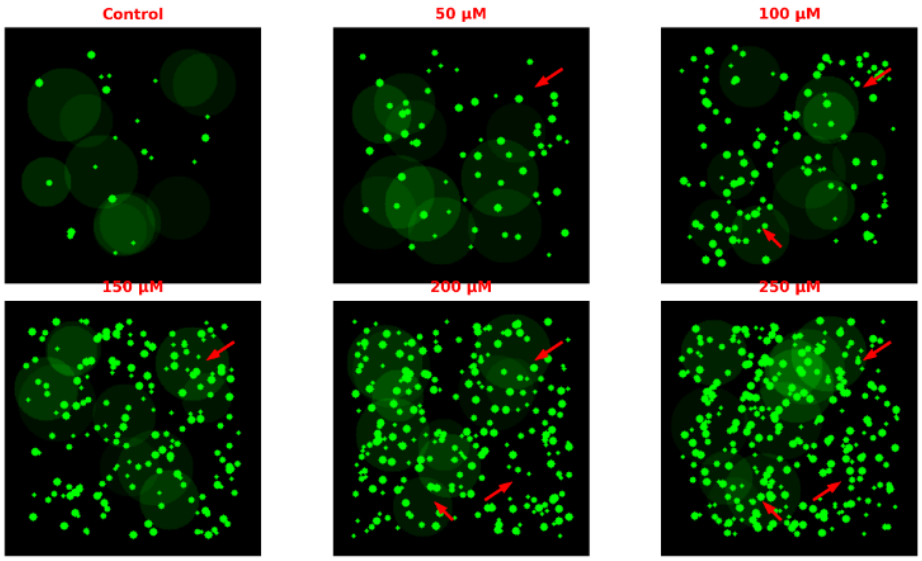

Figure 6. Dose-dependent effect of cells exhibits progressive morphological disruption.

The aggregation of fragmented signals and the reduction in intact fluorescence clusters confirm extensive cell membrane damage and loss of structural integrity. The red arrows highlight regions with visible fragmentation and disrupted cell clusters [28]. These findings demonstrate that the peptide exerts a dose-dependent cytotoxic effect, with lower concentrations initiating early membrane alterations and higher concentrations leading to pronounced cell lysis (Figure 7).

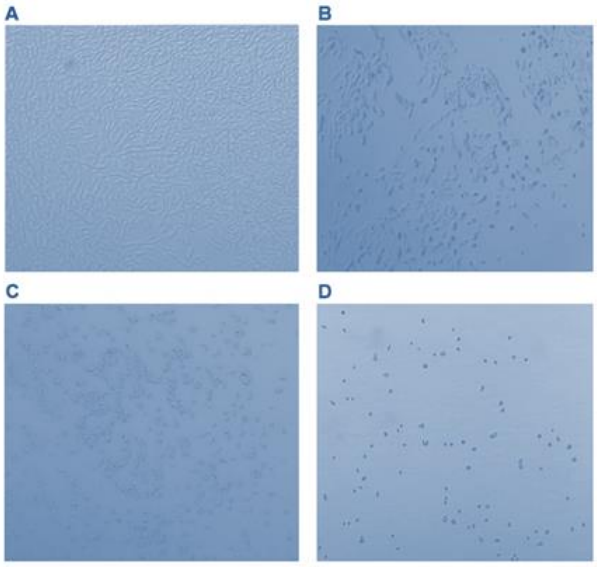

Figure 7. Dose-dependent peptide-induced membrane damage showing increased cell fragmentation and lysis from (A–D).

The untreated control group (Figure A) showed normal cell morphology, characterized by elongated, intact, and confluent growth with clear intercellular connections, indicating healthy and viable cells (Figure 8). Upon treatment with increasing concentrations of the peptide, a progressive loss of normal cell morphology was observed. At lower concentrations (Figure B), cells exhibited early signs of stress, including partial detachment, rounding, and reduced confluency [29]. With further increase in peptide concentration (Figure C), distinct cytopathic effects were evident, including cell shrinkage, aggregation, and marked detachment from the culture surface. At the highest concentration tested (Figure D), a pronounced cytotoxic effect was noted, with most cells appearing as rounded, shrunken structures scattered across the field, reflecting extensive cell death and lysis. These results suggest that the peptide induces dose-dependent cytotoxicity by disrupting cellular integrity and viability.

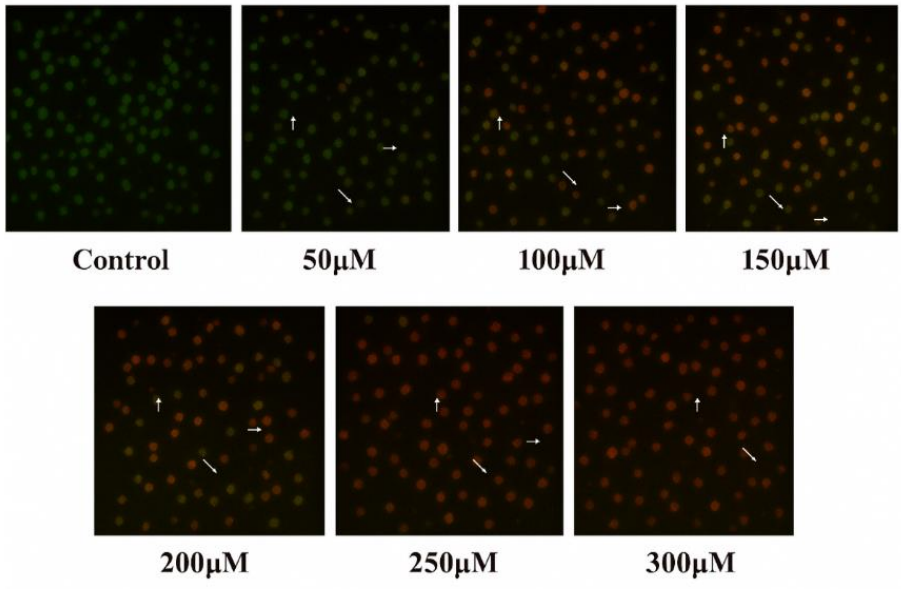

Figure 8. Dose-dependent cytotoxicity showing progressive loss of cell integrity and increased cell death with rising peptide concentrations (concentrations 50–300 μM).

In the control group, nearly all cells exhibited green fluorescence, indicative of intact viable cells with normal nuclear morphology. Upon treatment with 50 μM, a small population

of cells began to display orange/red fluorescence, accompanied by nuclear condensation and fragmentation (indicated by arrows), suggesting the initiation of apoptosis. As the concentration increased to 100 µM and 150 µM, a marked increase in apoptotic cell populations was observed, as evidenced by enhanced red/orange fluorescence and distinct nuclear morphological changes [30,31]. At higher concentrations (200–300 µM), the majority of cells exhibited intense red fluorescence, signifying loss of membrane integrity and late apoptotic or necrotic cell death. The progressive shift from green to orange/red fluorescence across concentrations clearly demonstrates a dose-dependent cytotoxic effect of the compound [32]. These findings confirm that the test compound induces apoptosis in a concentration-dependent manner, with lower doses initiating apoptotic signaling and higher doses driving cells toward complete apoptotic/necrotic death. The comet assay revealed a dose-dependent increase in DNA damage upon treatment with the test compound (Figure 9).

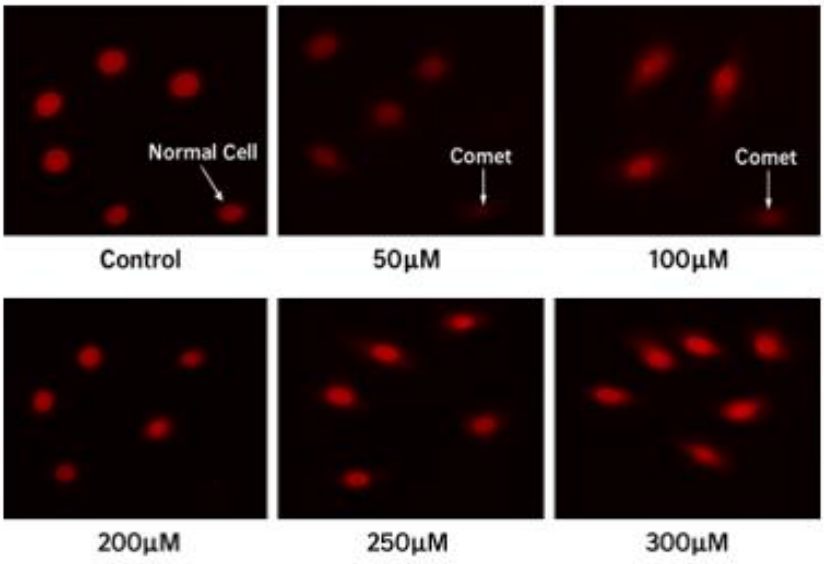

Figure 9. Comet assay showing dose-dependent DNA damage, with increased comet tail formation at higher peptide concentrations, indicating enhanced genotoxic stress.

The comet assay revealed a dose-dependent increase in DNA damage upon treatment with the test compound. In the control group, cells exhibited intact, spherical nuclei with no visible comet tails, confirming the absence of DNA fragmentation. At 50 µM concentration, the initial appearance of comet tails indicated mild DNA strand breaks. This effect intensified at 100 µM, with more cells displaying longer comet tails suggestive of moderate DNA damage. Interestingly, at 200 µM, a comparatively reduced DNA migration pattern was observed, possibly due to differential cellular response at this concentration [33]. However, at 250 µM and 300 µM, prominent comet tails reappeared, with increased tail length and intensity, indicating significant DNA fragmentation and genotoxic stress at higher concentrations [34]. These findings suggest a genotoxic potential of the compound at higher doses, which could be linked to mechanisms of direct interaction with nuclear DNA.

4. Conclusions

It is concluded that peptides extracted from *Cissus quadrangularis* (L.) were successfully isolated, purified, and characterized through a multistep approach combining gel filtration, ammonium sulfate precipitation, dialysis, and preparative HPLC. A dominant peptide fraction was identified, with a molecular ion peak at m/z 650.229, corresponding to a molecular weight of 650 Da, as confirmed by mass spectrometry. FTIR and CD analyses

validated the peptide nature and revealed characteristic amide functional groups with a predominant β-sheet secondary structure. Functional assays demonstrated strong dose-dependent cytotoxicity against CAL 27 cells, with progressive morphological alterations, loss of membrane integrity, and apoptotic features confirmed by fluorescence staining. DNA fragmentation analysis using the comet assay further highlighted the peptide's genotoxic and apoptotic potential at higher concentrations. Collectively, it is concluded that *C. quadrangularis* contains a major bioactive peptide with significant anticancer activity, warranting further in vivo validation and mechanistic investigations for therapeutic application.

Author Contributions

Conceptualization, S.K. and J.R.; methodology, J.R.; software, J.R.; validation, J.R., M.R., and P.A.; formal analysis, M.R.; investigation, S.K.; resources, S.K.; data curation, P.A.; writing-original draft preparation, M.R.; writing-review and editing, M.R.; visualization, M.R.; supervision, S.K.; project administration, J.R.; funding acquisition, J.R. All authors have read and agreed to the published version of the manuscript.

Institutional Review Board Statement

Not applicable.

Informed Consent Statement

Not applicable.

Data Availability Statement

Data supporting the findings of this study are available upon reasonable request from the corresponding author.

Funding

This research received no external funding.

Acknowledgments

We would like to thank the Department of Biotechnology, M.G.R. College, Hosur, and the Department of Microbiology, K.R. College of Arts and Science, Kovilpatti, for their valuable and supportive contributions to this publication.

Conflicts of Interest

The authors declare no conflict of interest.

References

1. Prasad, G.P.; Pratap, G.P.; Meenakshi, V.; Pal, P.K.; Srikanth, N. Ethnomedicinal and dietary uses of Cissus quadrangularis L. (Asthishrinkhala) from the tribes, rural people and traditional healers of Andhra Pradesh, India. J. Drug Res. Ayurvedic Sci. 2018, 3, 96–105. https://doi.org/10.5005/jp-journals-10059-0041
2. Li, Q.; Wang, Y.; Zhou, H.; Liu, Y.; Gichuki, D.K.; Hou, Y.; Zhang, J.; Aryal, R.; Hu, G.; Wan, T.; Amenu, S.G.; Gituru, R.W.; Xin, H.; Wang, Q. The *Cissus quadrangularis* genome reveals its adaptive features in an arid habitat. *Hortic. Res.* **2024**, *11*, uhae038, https://doi.org/10.1093/hr/uhae038.

3. Praneetha, S.; Kousalya, R.; Kamaleshwaran, N.K.; Kalaivani, P.; Kamaraju, A. Value added products of veldt grape (*Cissus quadrangularis*) and their organoleptic evaluation. *Madras Agric. J.* **2024**, *111*.
4. Hamid, H.S.; Patil, S. A Phytochemical and Pharmacological Review of an Indian Plant: *Cissus quadrangularis*. *Med. Sci. Forum* **2023**, *21*, 20, https://doi.org/10.3390/ECB2023-14557.
5. Kaur, J.; Dhiman, V.; Bhadada, S.; Katare, O.P.; Ghoshal, G. LC/MS guided identification of metabolites of different extracts of Cissus quadrangularis. *Food Chem. Adv.* **2022**, *1*, 100084,https://doi.org/10.1016/j.focha.2022.100084.
6. Zaki, S.; Chaithra, M.L.; Bansal, S.; Latha, V.; Bajpai, M.; Malathi, R.; Sibi, G. In vitro anti-inflammatory, anti-diabetic and antioxidant potential of Cissus quadrangularis along with its orexigenic activity in Drosophila melanogaster. *J. Appl. Nat. Sci.* **2021**, *13*, 962, https://doi.org/10.31018/jans.v13i3.2835.
7. Paul, S.; Das, P.K.; Saha, S.; Dhiwar, P.S.; Khanra, R.; Chatterjee, A.; Zanchi, F.B. Exploration of Antidiabetic and Anti-Apoptotic Activity of *Cissus quadrangularis* Stem Through Mechanistic Pathway: An *in vitro*, *in silico* and *in vivo* Approach. *Appl. Biochem. Biotechnol.* **2025**, *197*, 6507-6529, https://doi.org/10.1007/s12010-025-05338-6.
8. Farjana, H.N.; Valiathan, G.M.; Mohanasatheesh, S. In-silico study on biomolecules derived *from Cissus quadrangularis* towards anti-inflammation. *J. Genet. Eng. Biotechnol.* **2025**, *23*, 100571, https://doi.org/10.1016/j.jgeb.2025.100571.
9. Mondal, I.; Zilani, M.N.H.; Lisany, N.F.; Yasmin, F.; Bibi, S.; Biswas, P.; Tauhida, S.J.; Rahman, M.S.; Albadrani, G.M.; Al-Ghadi, M.Q.; Sayed, A.A.; Hasan, M.N.; Abdel-Daim, M.M. *Cissus quadrangularis* Revealed as a Potential Source of Anti-Inflammatory and Anti-Diabetic Pharmacophore in Experimental and Computational Studies. *Chem. Biodivers.* **2025**, *22*, e00903, https://doi.org/10.1002/cbdv.202500903.
10. Neha, D.; Shiv Shankar, S.; Ravindra Kumar, P.; Sagar, S.; Bina, G. Preparation, Optimization, and Characterization of Transdermal Patches Containing Aqueous Extract of *Cissus quadrangularis* and *Ginger officinalis*. *Curr. Nutr. Food Sci.* **2025**, *21*, 899-909, https://doi.org/10.2174/0115734013300898241011063621.
11. Sundhararajan, R.; Dhanalakshmi, A.; Latha, S.; Lokesh, S.; Manibharathi, K.; Megala, S.; Mohamed Adhil, A. Evaluation of In-vitro Anti-arthritic activity in Methanol and Acetone Extract of Stem of Cissus quadrangularis. *Int. J. Res. Pharm. Allied Sci.* **2025**, *4*, 89-94, https://doi.org/10.71431/IJRPAS.2025.4312.
12. Patcharin, S.; Anussara, K.; On-Anong, S.; Ruhainee, T. Comparative Phytochemical, Antioxidant, and Antibacterial Study of Different Solvent Extracts of Cissus hastata Leaves. *Pharmacogn. J.* **2025**, *17*, 511-519, https://doi.org/10.5530/pj.2025.17.64.
13. Mathangi, R.; Devarajan, N.; Lakshmi, U.D. An Overview of the Osteogenic potential of Indian herb Cissus quadrangularis (Veldt Grape). *South East. Eur. J. Public Health* **2024**, 2210-2214, https://doi.org/10.70135/seejph.vi.2354.
14. Dadge, S.D.; Syed, A.A.; Husain, A.; Valicherla, G.R.; Gayen, J.R. Simultaneous Estimation of Quercetin and *trans*-Resveratrol in *Cissus quadrangularis* Extract in Rat Serum Using Validated LC-MS/MS Method: Application to Pharmacokinetic and Stability Studies. *Molecules* **2023**, *28*, 4656, https://doi.org/10.3390/molecules28124656.
15. Nair, A.R.; Rajula, P.B.; Geddam, S.S.S.; Subhashini, B.; Lochini, S. Antibacterial Activity of *Cissus quadrangularis* (Veldt Grape) Against Porphyromonas gingivalis, a Keystone Pathogen in Periodontal Disease: An In Vitro Study. *Cureus* **2024**, *16*, e66377, https://doi.org/10.7759/cureus.66377.
16. Benjawan, S.; Nimitphong, H.; Tragulpiankit, P.; Musigavong, O.; Prathanturarug, S.; Pathomwichaiwat, T. The effect of *Cissus quadrangularis* L. on delaying bone loss in postmenopausal women with osteopenia: A randomized placebo-controlled trial. *Phytomedicine* **2022**, *101*, 154115, https://doi.org/10.1016/j.phymed.2022.154115.
17. Kontham, G.R.; Vutukuru, G.V.K.; Chepuri, K.; Chittepu, P.; Kathuroju, H.; Vadakavila, G.; Addepally, U.; Vutukuru, S.S. In vitro Assessment of the Antioxidant and Cytotoxic Activities of Cissus quadrangularis Using HeLa Cells. *Asian J. Biol. Life Sci.* **2024**, *13*, 760-769, https://doi.org/10.5530/ajbls.2024.13.92.
18. Mohandoss, K.; Vijayan, V.; Hemalatha, S. Cissus quadrangularis Phytosomes' Bioactivity Assessment: Cytotoxic, Anti-Inflammatory and Antioxidant Properties. *Asian J. Biol. Life Sci.* **2024**, *13*, 714-722, https://doi.org/10.5530/ajbls.2024.13.87.
19. Na Takuathung, M.; Aisara, J.; Sawong, S.; Koonrungsesomboon, N. The effects of *Cissus quadrangularis* on bone-related biomarkers in humans: a systematic review and meta-analysis. *BMC Complement. Med. Ther.* **2025**, *25*, 286, https://doi.org/10.1186/s12906-025-04995-8.

20. Vinoth, K.; Kumar, S.R. Morphological, molecular, and pharmacological review of veldt grape (*Cissus quadrangularis* L.): an underutilized medicinal plant. *Front. Plant Sci.* **2025**, *16*, 1586624, https://doi.org/10.3389/fpls.2025.1586624.
21. Farjana, H.N.; Valiathan, G.M. *Cissus quadrangularis*: A comprehensive review as an emerging biomaterial for periodontal regeneration. *J. Oral Res. Rev.* **2025**, *17*, 87–92, https://doi.org/10.4103/jorr.jorr_27_24.
22. Tiwari, M.; Gupta, P.S.; Sharma, N. Ethnopharmacological, phytochemical and pharmacological review of plant Cissus quadrangularis L. *Res. J. Pharmacogn. Phytochem*. **2018**, 10, 81–90. https://doi.org/10.5958/0975-4385.2018.00014.6.
23. Jyanthi, M.; Akash, A.; Akhil, S.; Pragathy, S.; Nandhakumar, G. Comprehensive review on botany, phytochemistry, pharmacology and its uses of Cissus quadrangularis. *Int. J. Agric. Food Sci.* **2025**, 7, 1163–1166. https://doi.org/10.33545/2664844X.2025.v7.i8k.687.
24. . Patil, A.M.; Pawar, A.B.; Purane, L.M.; Redasani, V.V. Therapeutic potential and pharmacological insights of Cissus quadrangularis Linn.: A comprehensive review. *Int. J. Pharmacogn*. **2025**, 12, 272–281. https://doi.org/10.13040/IJPSR.0975-8232.IJP.12(4).272-81
25. Sawangjit, R.; Puttarak, P.; Saokaew, S.; Chaiyakunapruk, N. Efficacy and safety of Cissus quadrangularis L. in clinical use: A systematic review and meta-analysis of randomized controlled trials. *Phytother. Res*. **2017**, 31, 555–567. https://doi.org/10.1002/ptr.5783
26. Das, A.; Dey, J.; Saha, A.; Choudhury, R.; Borah, S. Cissus quadrangularis Linn.: An ethnomedicinal plant with multisystem therapeutic potential and global relevance. RGU J. Soc. Sci. Res. 2025, 1, 188–200. https://doi.org/10.3254/rgujssr.v1i4.99
27. Charoensup, N.; Sangthong, K.; Kongcharoen, W. Cissus quadrangularis in bone healing and oxidative stress. *J. Adv. Med. Pharm. Sci*. **2024**, 3, 1–10. https://doi.org/10.36079/lamintang.jamaps-0301.585
28. Na Takuathung, M.; Aisara, J.; Sawong, S.; Koonrungsesomboon, N. The effects of Cissus quadrangularis on bone-related biomarkers in humans: A systematic review and meta-analysis. BMC Complement. Med. Ther. **2025**, 25, 286. https://doi.org/10.1186/s12906-025-04995-8
29. Narayanan, L.; S.R., S. Pharmacological insights into Ipomoea staphylina: Therapeutic activities and the isolated bioactive metabolic compounds. *Mong. J. Chem.* **2024**, 25, 52. https://doi.org/10.5564/mjc.v25i52.3195
30. Vinoth, K.; Kumar, S.R. Morphological, molecular, and pharmacological review of veldt grape (Cissus quadrangularis L.): An underutilized medicinal plant. *Front. Plant Sci*. **2025**, 16, 1586624. https://doi.org/10.3389/fpls.2025.1586624.
31. Jagat, R.K.; Rupinder, K.K.; Hannah, B.; Sara, B. Recent Advances on the Roles of NO in Cancer and Chronic Inflammatory Disorders. *Curr. Med. Chem.* **2009**, *16*, 2373-2394, https://doi.org/10.2174/092986709788682155.
32. Bhujade, A.M.; Talmale, S.; Kumar, N.; Gupta, G.; Reddanna, P.; Das, S.K.; Patil, M.B. Evaluation of *Cissus quadrangularis* extracts as an inhibitor of COX, 5-LOX, and proinflammatory mediators. *J. Ethnopharmacol.* **2012**, *141*, 989-996, https://doi.org/10.1016/j.jep.2012.03.044.
33. Parisuthiman, D.; Singhatanadgit, W.; Dechatiwongse, T.; Koontongkaew, S. *Cissus quadrangularis* extract enhances biomineralization through up-regulation of MAPK-dependent alkaline phosphatase activity in osteoblasts. *In Vitro Cell. Dev. Biol.-Animal* **2009**, *45*, 194-200, https://doi.org/10.1007/s11626-008-9158-1.
34. Potu, B.K.; Rao, M.S.; Nampurath, G.K.; Chamallamudi, M.R.; Prasad, K.; Nayak, S.R.; Dharmavarapu, P.K.; Kedage, V.; Bhat, K.M.R. Evidence-based assessment of antiosteoporotic activity of petroleum-ether extract of Cissus quadrangularis Linn. on ovariectomy-induced osteoporosis. *Upsala J. Med. Sci.* **2009**, *114*, 140-148, https://doi.org/10.1080/03009730902891784.

Publisher's Note & Disclaimer

information before relying on it, and the publisher assumes no responsibility for any consequences arising from the use of materials contained in this publication.